

Integrating Independent Component Analysis with Artificial Neural Network to Analyze Overlapping Fluorescence Spectra of Organic Pollutants

Ling Gao · Shouxin Ren

Received: 16 May 2012 / Accepted: 20 June 2012 / Published online: 5 July 2012
© Springer Science+Business Media, LLC 2012

Abstract Independent component analysis (ICA) combined with Elman recurrent neural network (ERNN) regression as a hybrid approach named ICA-ERNN was proposed for the simultaneous spectrofluorimetric determination of organic pollutants. Fluorescence spectra of these compounds under study are strongly overlapped, which does not permit direct determination without prior separation by conventional spectrofluorimetry. ICA is a blind source separation (BSS) method aiming at extracting independent source variables and their corresponding concentration profiles from the observed fluorescence spectra of chemical mixtures without using any prior knowledge about the components. The proposed method combining the idea of ICA denoising with ERNN calibration provides the ability for enhancing the extraction of characteristic information and the noise removal as well as the quality of regression. The relative standard errors of prediction (RSEP) obtained for all components using ICA-ERNN, ERNN and partial least squares (PLS) were compared. Experimental results demonstrated that the ICA-ERNN method had better result than ERNN and PLS methods and was successful even when there was severe overlap of fluorescence spectra.

Keywords Independent component analysis · Elman recurrent neural network · Spectrofluorimetry · Organic pollutants · Multicomponent determination

Introduction

Spectrofluorimetry has been widely used in biological and environmental analysis because it is simple, rapid, and has

high sensitivity, moderate selectivity and relatively low cost. In complex samples, however, the presence of fluorescence spectral overlap of multi-components hinders the determination of several compounds in their mixtures by conventional method without prior separations. Nowadays, due to the easy and fast acquisition of data, chemometric methods have been widely applied to solve the problem of overlapping signals [1–6]. Researchers seek to use chemometric techniques to maximize the information obtained from raw data. Several chemometric methods such as principal component analysis (PCA) and partial least squares (PLS) have recently emerged as fast growing techniques; however, comparing to spectrometry, there are only a few references to chemometric methods dedicated to fluorescence spectral problems [7, 8]. Recently, Considerable interest has arisen regarding the independent component analysis (ICA) techniques [9, 10] that specifically address the areas such as medical signal analysis, image process, speech recognition, fault detection, statistical process monitoring and analytical data analysis [11–13]. ICA is a newly developed signal processing technique aiming at solving related blind source separation (BSS) problem. ICA can be used to extract independent source variables and their corresponding concentration profiles from the observed fluorescence spectra of chemical mixtures without using any prior knowledge about the components under the assumption that source variables are statistically independent. Being commonly considered as a further development of principal component analysis (PCA), the ICA model is similar to PCA. The main difference between ICA and PCA is that the ICA finds independent and non-Gaussian independent components (ICs) and the PCA finds orthogonal principle components (PCs). In probability theory, independent is a high-order statistic. Thus, ICA involves high-order statistics with no orthogonal constraint and is considered to be more powerful in the multivariate data analysis. Like PCA, ICA has already been used as a pretreatment method in order to reduce fluorescence

L. Gao · S. Ren (✉)
Department of Chemistry, Inner Mongolia University,
Huhhot 010021 Inner Mongolia, People's Republic of China
e-mail: cersx@mail.imu.edu.cn

spectra dimension and to avoid redundancy information. These characteristics of ICA make it possible to make dimension reduction and to extract ICs and mixing matrix from observed complex fluorescence spectra. The mixing matrix resulted from the ICA represents the relative concentration level of the ICs. The model of the mixing matrix and concentration matrix was built by ERNN regression. Artificial neural network (ANN) is one of the most broadly used mathematical algorithms for regression problems [14]. ANN is a mathematical model of which composition is inspired by the structure of human brain. Recently, it has been proposed that ANN can be used to solve regression problems by acting as non-parametric calibration methods, which have the ability to learn from a set of examples without requiring any knowledge of the model type and generalize this knowledge to new situations [15, 16]. ANN has the outstanding power for modeling both linearity and non-linearity systems. Presently the most widely used ANN is a multilayer feedforward network (MLFN) with back propagation algorithm (BP). However, the BP-MLFN method often has the deficiency of slow convergence, is prone to the existence of many local minima during training, and tends to overfit. Much attention has been paid to solve these problems and to facilitate the training process into the global minimum. An ANN called Elman recurrent neural network (ERNN) was used in this case. It was introduced into the ANN literature by J.L. Elman in 1990 [17]. A recurrent neural network (RNN) has recurrent links between its layers and uses these links to provide networks with dynamic memory. In the Elman network, a so-called context layer, which provides the network with memory, is added to the conventional feedforward neural network. The RNN is able to tackle the linear and non-linear relationships between fluorescence spectra and concentrations and reduce the computational complexity of the training procedure. Until now, RNN has rarely been applied to analytical chemistry [18]. In this case, an ICA based ERNN regression (ICA-ERNN) method was developed to perform simultaneous spectrofluorimetric determination. The approach of ICA combined with ERNN seems to be the first application to the simultaneous spectrofluorimetric determination of biphenyl, naphthalene and benzotriazol, which are highly toxic and have carcinogenic effects. Therefore, it is very important to detect and monitor biphenyl, naphthalene and benzotriazol in biological and environmental samples. These factors have led to develop newer and faster analytical methods combining chemometrics and spectrofluorimetry for improved selectivity and sensitivity. The proposed method was successfully applied to the simultaneous determination of biphenyl, naphthalene and benzotriazol mixtures in which their fluorescence spectra are overlapped. Its ability of improving the performance of simultaneous multicomponent determination was clearly demonstrated.

Theory

Independent Component Analysis

ICA is a statistical data processing technique that aims to decompose observed analytical signals derived from multicomponent mixture into pure signals and their concentration profiles under the assumption that the source signals are statistical independent. ICA can be expressed as the following:

$$X = AS \quad (1)$$

Where X is $m \times n$ observed data matrix, S is $k \times n$ independent source matrix, and A is $m \times k$ data matrix of unknown concentrations, called the mixed matrix. Here m is the number of observed mixture, n denotes the number of counts over wavelength and k is the number of independent components. The goal of the ICA is to estimate the mixing matrix A and independent source matrix S from the observed data matrix. The problem is finding the unmixing matrix W such that $S = WX$. When W is an inverse of the mixing matrix A , the estimated independent source signals should equal to the original independent source signals. The most task of ICA is to find out the unmixing matrix W based on the principle that the estimated S independent source signals become as independent of each other as possible. Thus, the task turns into an optimization problem under the constraints of independency. A large number of ICA algorithms [19, 20] have been proposed including FastICA, joint approximate diagonalization of eigenmatrices (JADE), Infomax, Kernel ICA (KICA) and mean field ICA (MF-ICA). In this paper the JADE algorithm is applied to perform ICA operation. The JADE algorithm uses joint diagonalization of a set of fourth-order cumulant matrices. For the details of JADE algorithm please refer to references of this paper [21, 22]. In the first step of the JADE-ICA algorithm, the observed data matrix X has been whitened to remove any correlation among random variables. One popular method for whitening is to use the eigenvalue decomposition (EVD) of the covariance matrix of X [9]. Whitening also can reduce the complexity of the problem.

Elman Recurrent Neural Network

ERNN consists of four layers—the input layer, the context layer, the hidden layer and the output layer. The input layer does not process information; it serves only to distribute input data among the hidden layers. The input layer is the first layer with one node for each variable that is representative of the characteristics of the problem. The hidden layer is essentially the same for MLFN, which receives input data and is responsible for processing the data. The number of hidden nodes is an adjustable parameter. In the hidden layer a non-linear hyperbolic tangent sigmoid function is used as the transfer

function. In general, there are fewer nodes in the hidden layer than in the input layer; the transformation from input to hidden layer represents a dimensionality reduction. The last layer is the output layer consisting of one node for each variable to be investigated. In output layer a linear transfer function is used. In this case, output layers output predicted concentrations of the three kinds of analytes. Similar to regular feedforward neural networks, signals are propagated from the input layer through the hidden layer to the output layer. The peculiarity of ERNN is having the context layer, which is a special case of the hidden layer. The context layer interacts only with nodes in the hidden layer and not with those in input or output layers. Nodes in the context layer depend only on the activation of nodes in hidden layer from the previous input. The Elman network has exactly the same number of nodes in the hidden and context layers. The output of each node in the hidden layer has individual copy in the context layer. The value of context node is used as an extra input signal for all the nodes in hidden layer for the next step. For this reason, the context layer provides the network with memory from the previous iteration. In the forward connection, the context layer is a group of internal input nodes and acts like input layer, whereas in the feedback connections the context layer can provide the network with dynamic memory.

The simple architecture of an ERNN is shown in Fig. 1. The dynamics of ERNN are described by the difference equation:

$$X_h(k + 1) = S\{W_c X_c(k + 1) + W_I U(k)\} \tag{2}$$

$$X_c(k + 1) = W_r X_h(k) \tag{3}$$

$$Y(k + 1) = W_o X_h(k + 1) \tag{4}$$

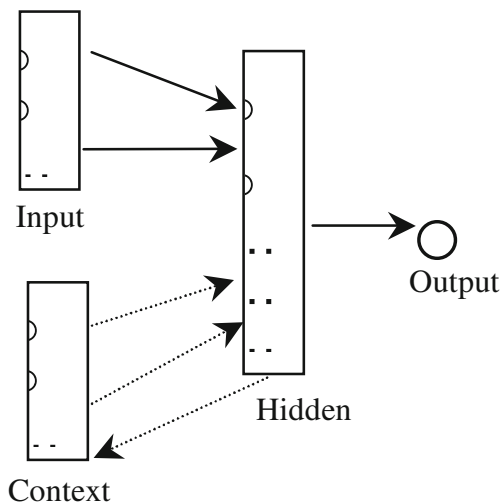


Fig. 1 Simple plot of the ERNN architecture

where S is a hyperbolic tangent function; $U(k)$ and $Y(k)$ are the input and the output of the network at a discrete time k ; X_c and X_h are the nodes of the context and the hidden layers; W_c , W_I , W_r and W_o are the weight matrices for the context-hidden, input-hidden, hidden-context and hidden-output layer interfaces, respectively. In general, the weights from the hidden layer to the context layer, W_r , are set to unity; i.e., after the outputs of the hidden nodes have been computed, these current values are copied exactly into the corresponding context nodes via the recurrent connection for the next time step. Thus, the context layer provides the network with memory from previous iterations. Training of the Elman network is performed by the fast back-propagation algorithm.

ICA-ERNN Arithmetic Algorithm

The ICA-ERNN algorithm can be summarized as follows:

1. The whole set of fluorescence spectra obtained from standard mixtures is used to build the experimental data matrix D .
2. The matrix D is decomposed into the mixing matrix A and independent source matrix S . The matrix S , which is also called the independent components of the observed data, are assumed to be non-Gaussian and mutually independent. Here, independence means the information carried by one component cannot carry any information from the others. Statistically this means that the joint probability is obtained as the product of the probability of each of them. A is the mixing matrix of weighting coefficients related to the corresponding concentrations. The mixing matrix A , derived from ICA, was used as input data to ERNN.
3. ERNN was proposed for generalizing the regression model in order to calibrate between its inputs and the desired outputs. The mixing matrix A , derived from ICA, was used as input data to the ERNN. ERNN can be trained with gradient descent back-propagation (BP). Here, a fast algorithm was selected as a suitable algorithm so that a more complex and computationally expensive algorithm was not required.

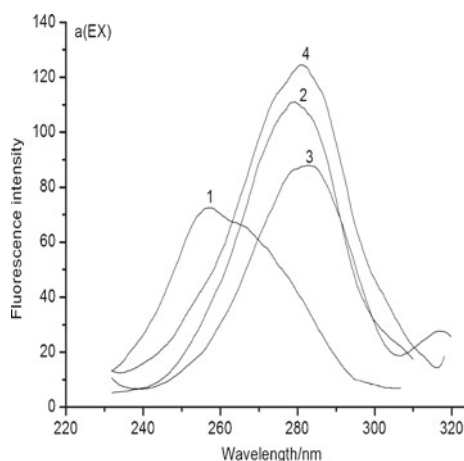
A programs PICAERNN was designed to perform the simultaneous spectrofluorimetric multicomponent determination.

Experimental

Apparatus and Reagents

All experiments was performed on a RF-5301 PC fluorescence spectrophotometer(Shimadzu,Japan), equipped with a 150 W Xenon lamp. A Lenovo Pentium IV microcomputer was used for all calculations. pH

Fig. 2 Excitation spectra of 1: biphenyl ($1.2 \mu\text{g mL}^{-1}$) 2: naphthalene ($1.2 \mu\text{g mL}^{-1}$) 3: benzotriazol ($12 \mu\text{g mL}^{-1}$) 4: their mixture



Excitation spectra of 1: biphenyl ($1.2 \mu\text{g mL}^{-1}$) 2: naphthalene ($1.2 \mu\text{g mL}^{-1}$) 3: benzotriazol ($12 \mu\text{g mL}^{-1}$) 4: their mixture

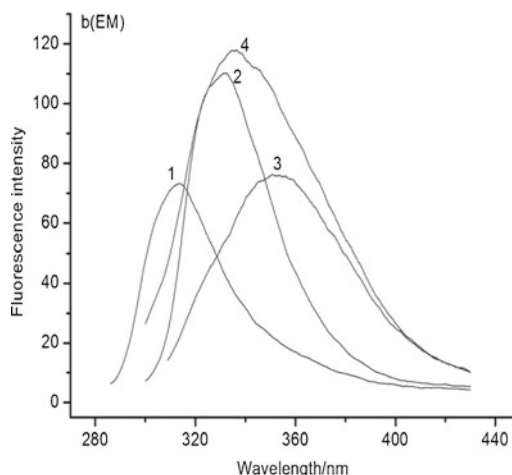
measurements were made with a pH-3B digital pH meter with a glass-saturated calomel dual electrode. All reagents were of analytical reagent grade. Doubly distilled and deionized water was used. Stock standard solutions of 1 gL^{-1} of biphenyl, naphthalene and benzotriazol were prepared from correspondent reagents with alcohol and water as solvents. Standard solutions were then prepared from the stock standard solutions by serial dilution as required. pH=6.50 Britton-Robinson buffer solution was prepared by sodium hydroxide and mix acids (phosphoric acid, acetic acid and boric acid).

Procedure

A series of mixed standard solutions containing various ratios of biphenyl, naphthalene and benzotriazol was

prepared in 25 mL standard flasks; 5.00 mL of Britton-Robinson buffer solution (pH=6.50) were added and diluted with distilled water to the mark. The solutions were placed in the quartz cuvettes with a path length of 1 cm. With excitation wavelength of 275 nm, fluorescence emission spectra were measured between 290.0 nm and 430.0 nm at 0.2 nm intervals. Experimental data were saved in ASCII format and transformed to a personal computer for succeeding utilization. The whole set of fluorescence emission spectra obtained in 16 standard mixtures was used to build up the matrix D. Using the same procedures, a D_u matrix for unknown mixtures was built up. Experimental conditions used for fluorescence spectra were as follows: scan rate, high; excitation wavelength, 275 nm; excitation and emission slit widths, 10 nm; sensitivity, high.

Fig. 3 Emission spectra of 1: biphenyl ($1.2 \mu\text{g mL}^{-1}$) 2: naphthalene ($1.2 \mu\text{g mL}^{-1}$) 3: benzotriazol ($120 \mu\text{g mL}^{-1}$) 4: their mixture



Emission spectra of 1: biphenyl ($1.2 \mu\text{g mL}^{-1}$) 2: naphthalene ($1.2 \mu\text{g mL}^{-1}$) 3: benzotriazol ($120 \mu\text{g mL}^{-1}$) 4: their mixture

Table 1 ERNN training parameters

Training parameters	Value
Initial learning rate	0.001
Learning rate increase	1.05
Learning rate decrease	0.7
Momentum constant	0.95
Maximum error ratio	1.04
Performance goal (SSE)	0.0001

Results and Discussion

Absolute and relative standard errors of prediction (SEP and RSEP) were used as the criteria for comparing the performances of the test methods [4].

Excitation and Emission Spectra Characteristics

Figures 2 and 3 show at pH=6.50 the excitation spectra and the emission spectra of biphenyl, naphthalene and benzotriazol and their mixed solution, respectively. It can be seen from Figs. 2 and 3 that the excitation spectra and the emission spectra of these three compounds are seriously overlapped in the wavelength ranges. The Fig. 3 indicated that the maximum emission wavelengths of biphenyl, naphthalene and benzotriazol were 312 nm, 331 nm and 353 nm respectively. The emission spectra of their mixture were severely overlapped and exhibited only one peak for which maximum emission wavelength is at 338 nm. Thus, conventional fluorimetric methods cannot perform direct determination without previous separation.

Optimization of the Experimental Conditions

The optimal experimental conditions for this system were selected experimentally. The selection of excitation wavelength is

one of the most important steps for spectrofluorimetric analysis of multicomponent mixtures. Referring to the excitation spectra (Fig. 2), we selected the wavelength range of 220.0 nm and 320.0 nm as experimental range, in which each individual excitation spectrum was selected, respectively, then the effect of the different excitation wavelength on fluorescence intensities of emission spectra scanned were tested. After test, excitation wavelength 275 nm was determined. Fluorescence signals are very complex, likely to interference and scattering, and prone to overlap. In order to eliminate partly these effects, the selection of the wavelength range of emission spectra is very necessary. After trial, with excitation wavelength 275 nm, emission spectra wavelength range between 290.0 nm and 430.0 nm was chosen, since the three detected compounds have stable fluorescence intensities and include their whole information in this wavelength range as well as first-order and second-order Rayleigh scattering can be avoided. The effect of pH on this experimental system was evaluated over the range of pH 5.00~7.50. After trials, the biphenyl, naphthalene and benzotriazol had stable fluorescence intensity within the range of pH 5.25~7.50, 5.25~7.00 and 5.50~7.00, respectively. Therefore, buffer solution (pH=6.50) was used in this case. The influence of the amount of buffer solution on the fluorescence signals was investigated in the range of 1.00–6.00 ml, after examination, final volume 5.00 of the buffer solution was chose for providing adequate buffer capacity. The selections of instrumental parameters on this experimental system were also investigated. Selected optimal experimental conditions were the same as those described in experimental procedure.

An ICA-Based ERNN Regression

The judicious choice of network structure and process parameters plays an important role in successfully obtaining a reliable result by the ICA-ERNN method. Five parameters were optimized in the ICA-ERNN training: the number of ICs, number of hidden nodes, the initial learning rate, the momentum and the sum squared error (SSE) goal. The first one are

Table 2 Composition of the training set

Sample No.	Concentration ($\mu\text{g mL}^{-1}$)			Sample No.	Concentration ($\mu\text{g mL}^{-1}$)		
	I	II	III		I	I	III
1	0.200	0.120	0.960	9	1.000	0.120	7.200
2	0.200	0.600	4.800	10	1.000	0.600	9.600
3	0.200	1.000	7.200	11	1.000	1.000	0.960
4	0.200	1.400	9.600	12	1.000	1.400	4.800
5	0.600	0.120	4.800	13	1.400	0.120	9.600
6	0.600	0.600	0.960	14	1.400	0.600	7.200
7	0.600	1.000	9.600	15	1.400	1.000	4.800
8	0.600	1.400	7.200	16	1.400	1.400	0.960

I: biphenyl; II: naphthalene; III: benzotriazol

Table 3 Actual concentration and percentage recovery of the unknowns

Sample No.	Actual concentration ($\mu\text{g mL}^{-1}$)			Recovery (%) ICA-ERNN		
	I	II	III	I	II	III
1	0.400	0.400	2.400	107.6	79.7	101.9
2	0.400	0.800	6.000	99.9	99.8	100.4
3	0.400	1.200	8.400	119.1	100.1	99.5
4	0.800	0.400	6.000	104.4	76.1	100.5
5	0.800	0.800	8.400	105.9	87.7	100.4
6	0.800	1.200	2.400	120.1	94.3	97.3
7	1.200	0.400	8.400	102.0	70.3	100.7
8	1.200	0.800	2.400	111.6	110.4	94.6
9	1.200	1.200	6.400	78.7	101.1	103.4

I: biphenyl; II: naphthalene; III: benzotriazol

associated with ICA and the other four are required by the ERNN network. It is possible to use the predictive parameters SEP and RSEP to find the optimum choice of functions. ICA is a newly developed signal processing technique aiming at solving related blind source separation (BSS) problem. ICA focuses to decompose an observed mixture data into a linear mixture of a priori unknown source signals assuming that they are statistically independent. The mixing matrix, which represents the relative concentration level of the ICs, was obtained by the ICA. This proposed method combines ICA and ERNN regression to make dimension reduction and to extract ICs and mixing matrix from observed complex signals as well as to enhance the quality of the regression. Selection of the number of ICs is one of the most important steps that must be performed in ICA-based methods. In principle, the number of ICs is equal to the number of chemical components in the observed mixture data matrix. Thus, this number is a key parameter to ensure the correctness of this method. The mixing matrix *A*, resulted from ICA, was used as input data to ERNN. ERNN has the ability of learning from examples without any knowledge of the model type. In ERNN, the so-called context layer was added to the conventional feed forward neural network and provides the network with memory. The context layer interacts only with the nodes of the hidden layer and not with the input and output layers. The feedback loops pass from the output of the hidden layer to the context

Table 4 RSEP values for biphenyl, naphthalene and benzotriazol system by the three methods

Methods	RSEP (%)			
	I	II	III	Total compounds
ICA-ERNN	13.4	8.74	1.46	2.64
ERNN	18.9	27.1	4.96	6.68
PLS	15.3	11.4	9.92	10.1

I: biphenyl; II: naphthalene; III: benzotriazol

layer. The context layer simply holds a copy of the activations of the hidden layer from the previous step and provides the network with memory. In fact, ERNN is an extension of MLFN, and like MLFN the optimal architecture and parameters must be chosen. The transfer functions for the nodes in the hidden and output layer are hyperbolic tangent functions and linear functions, respectively. ANN utilizes the weight matrices to perform mathematical transformation of the input vector into the output vector. The process of adapting the weights to optimum values is called training. The training of a neural network is a numerical search for the minimum in an error cost function. In this case, the sum squared error (SSE) function is used as the criterion when monitoring the training process. The training is usually stopped when the network reaches predefined SSE goal. As training progresses, the SSE is calculated after a certain number of epochs. A statistical graph of the SSE against the epochs was plotted while monitoring the progress of training. A number of learning algorithms can be used to train a neural network. The fast back-propagation of errors learning algorithm was used in this case. Since the input and output of the network are fixed by the problem studied, the only layer of which size was yet to be determined was the hidden layer. There is no theoretical rule concerning the choice of the number of hidden nodes, since this parameter depends on the complexity of the problem. The selection of nodes in hidden layers was empirical; 1 to 16 hidden nodes were tested. The lowest SEP value was obtained with 8 hidden nodes. Thus, 8 is the optimal number of hidden layer nodes. A self-adaptive learning rate and a momentum term were employed in the fast back propagation algorithm. If the learning rate was too large, the network would become unstable and the results were of either high prediction error or bad convergent behavior. On the other hand, if the learning rate was too small, the training time would be excessively long. The fast BP algorithm has the ability to self-adjust the learning rate. The adaptive learning rate will attempt to keep the learning rate as large as possible while keeping the learning stable. Thus, the learning rate is varied automatically

according to whether or not the error ratio of new to old error is more than a fixed maximum error ratio as the training progresses. The initial learning rate and other training parameters were selected to improve the quality of the training by trial and error. The training parameters are shown in Table 1. The momentum constant gives the learning process a certain capacity for inertia and enables the network to avoid partial minima efficiently. The momentum constant was adjusted from 0.10 to 1.00. The relation between the RSEP and the momentum constant was calculated for all components. It was found that when the momentum value was 0.95, the RSEP showed fewer errors, and the network achieved faster convergence. After trials, the number of ICs=3, the number of hidden nodes=8, initial adapted learning rate=0.001, momentum=0.95 and the SSE goal=0.0001 were selected as optimal parameters.

A training set of 16 samples formed by the mixture of biphenyl, naphthalene and benzotriazol was designed according to four-level orthogonal array design with the $L_{16}(4^5)$ matrix. Table 2 summarizes the composition of the training set. The fluorescence emission spectra were measured between 290 nm and 430 nm at 0.2 nm intervals using 275 nm as the excitation wavelength. The whole set of fluorescence emission spectra obtained in 16 standard mixtures was used to build up the matrix D. A set of 9 synthetic unknown samples were measured in the same way as the training set and arranged in matrix D_u . Using program PICAERNN, the concentrations of biphenyl, naphthalene and benzotriazol for a test set were calculated and actual concentrations and recoveries of each component are listed in Table 3. All the experimental values in Table 3 were means of three replicates. The experimental results showed that the RSEP for all components were 2.64 %.

A Comparison of ICA-ERNN, ERNN and PLS Methods

In order to evaluate the ICA-ERNN method, three methods (ICA-ERNN, ERNN and PLS) were tested in the study with a set of synthetic unknown samples. The RSEP for the three methods are given in Table 4. The RSEP for all components with ICA-ERNN, ERNN and PLS were 2.64 %, 6.68 % and 10.1 %, respectively. From Table 4, it can be seen that ICA-ERNN is successful at the simultaneous spectrofluorimetric determination of overlapping peaks and can deliver better-calculated results than ERNN and PLS; the RSEP for all components were 2.64 %.

Conclusion

A method named ICA-ERNN was developed and employed to perform the automatic calculations for the simultaneous spectrofluorimetric determination of biphenyl, naphthalene and benzotriazol. Fluorescence spectra of these compounds

are strongly overlapped, which does not permit direct determination without prior separation by conventional spectrofluorimetry. The ICA-ERNN method relies on the concept of combining the idea of ICA denoising with ERNN calibration for enhancing the noise removal ability and the quality of regression. The proposed method combines ICA, which was used as a tool for reducing the dimension of raw fluorescence spectra and extracting information from the observed mixture spectra, and ERNN, which provides calibration model and performs for enhancing the quality of regression. This method overcomes the difficulty imposed by overlapping fluorescence spectra without prior separation. The method can efficiently reduce model complexity and at the same time enhance the performance of the calibration. The ICA-ERNN method has been shown to be a successful approach to the simultaneous spectrofluorimetric determination of biphenyl, naphthalene and benzotriazol and gives significantly improved performance of determination comparing with ERNN and PLS.

Acknowledgements The authors would like to thank National Natural Science Foundation of China (21067006 and 60762003) for financial support of this project.

References

1. Einax JW (2008) Chemometrics in analytical chemistry. *Anal Bioanal Chem* 390:1225–1226
2. Editorial (2008) Is there a future for chemometrics? Are we still needed? *Chemometr Intell Lab Syst* 191:99–100
3. Hasani M, Moloudi M, Emami F (2007) Spectrophotometric resolution of ternary mixtures of tryptophan, tyrosine, and histidine with the aid of principal component-artificial neural network models. *Anal Biochem* 370:68–76
4. Ren SX, Gao L (2000) Simultaneous quantitative analysis of overlapping spectrophotometric signals using wavelet multiresolution analysis and partial least squares. *Talanta* 50(6):1163–1173
5. Gao L, Ren SX (2005) Simultaneous spectrophotometric determination of four metals by two kinds of partial least squares methods. *Spectrochim Acta Part A* 61:3013–3019
6. Gao L, Ren SX (2010) Combining orthogonal signal correction and wavelet packet transform with radial basis function neural networks for multicomponent determination. *Chemometr Intell Lab Syst* 100:57–65
7. Bouveresse DJR, Benabid H, Rutledge DN (2007) Independent component analysis as a pretreatment method for parallel factor analysis to eliminate artefacts from multiway data. *Anal Chim Acta* 589:216–224
8. Kong X, Zhu W, Zhao Z, Li X, Wang H, Chen R, Chen C, Zhu F, Guo X (2012) Fluorescence spectroscopic determination of triglyceride in human serum with window genetic algorithm partial least squares. *J Chemometrics* 26:25–33
9. Hyvarinen A, Oja E (2000) Independent component analysis: algorithm and applications. *Neural Netw* 13:411–430
10. Lathauwer LD, Moor BD, Vandewalle J (2000) An introduction to independent component analysis. *J Chemometrics* 14:123–149
11. Brys G, Hubert M, Rousseeuw PJ (2005) A robustification of independent component analysis. *J Chemometrics* 19:364–375

12. Toivianen M, Corona F, Paaso J, Teppola P (2010) Blind source separation in diffuse reflectance NIR spectroscopy using independent component analysis. *J Chemometrics* 24:514–522
13. Wang G, Ding Q, Hou Z (2008) Independent component analysis and its application in signal processing for analytical chemistry. *Trends Anal Chem* 27:368–376
14. Marini F, Magri AL, Bucci R, Magri AD (2007) Use of different artificial neural networks to resolve binary blends of monocultivar Italian olive oils. *Anal Chim Acta* 599(2):232–240
15. Perez-Marin D, Garrido-varo A, Guerrero JE (2007) Non-linear regression methods in NIRS quantitative analysis. *Talanta* 72:28–42
16. Ren SX, Gao L (2004) Wavelet packet transform and artificial neural network applied to simultaneous kinetic multicomponent determination. *Anal Bioanal Chem* 378(5):1392–1398
17. Elman JL (1990) Finding structure in time. *Cognitive Science* 14:179–211
18. Lin CM, Huang JJ, Gen M, Tzeng GH (2006) Recurrent neural network for dynamic portfolio selection. *Appl Math Comput* 175:1139–1146
19. Hyvarinen A (1999) Survey on independent component analysis. *Neural Comput Survey* 2:94–128
20. Langlois D, Chartier S, Gosselin D (2010) An introduction to independent component analysis: InforMax and FastICA algorithm. *Tutorials Quant Meth Psychol* 6(1):31–38
21. Cardoso JF (1999) High-order contrasts for independent component analysis. *Neural Comput* 11:157–192
22. Cardoso JF, Souloumiac A (1993) Blind beamforming for non Gaussian signals. *IEEE Proc F* 140:362–370